Bull Eng Geol Environ
DOI 10.1007/s10064-009-0185-2

ORIGINAL PAPER

A case study from Koyulhisar (Sivas-Turkey) for landslide susceptibility mapping by artificial neural networks

Işık Yilmaz

Received: 28 October 2007 / Accepted: 26 October 2008

Abstract A case study for the use of an artificial neural network (ANN) model for landslide susceptibility mapping in Koyulhisar (Sivas-Turkey) is presented. Digital elevation model (DEM) was first constructed using ArcGIS software. Relevant parameter maps were created, including geology, faults, drainage system, topographical elevation, slope angle, slope aspect, topographic wetness index, stream power index, normalized difference vegetation index and distance from roads. Finally, a landslide susceptibility map was constructed using the neural networks. The drawbacks of the method are discussed but as the validation procedures used confirmed the quality of the map produced, it is recommended the use of ANN may be helpful for planners and engineers in the initial assessment of landslide susceptibility.

Keywords Landslide · Susceptibility · GIS · Artificial neural networks · Koyulhisar

Résumé Une étude de cas relative à l'utilisation d'un modèle de réseaux de neurones artificiels (ANN) pour la cartographie de la susceptibilité aux glissements de terrain à Koyulhisar (Sivas – Turquie) est présentée. Un modèle numérique de terrain (DEM) a d'abord été construit avec le logiciel ArcGIS. Les cartes de paramètres adéquates ont été créées, comportant la géologie, les failles, le système de drainage, les cotes topographiques, les pentes des terrains, la morphologie des pentes, l'indice d'humidité de surface, l'indice d'érosivité des cours d'eau, l'indice de végétation normalisé et les distances aux routes. Finalement, une carte de susceptibilité aux glissements a été construite à partir de réseaux de neurones. Les difficultés liées à ce type de méthode sont discutées mais, comme les procédures de validation utilisées ont confirmé la qualité de la carte produite, il est recommandé aux aménageurs et aux ingénieurs d'utiliser l'ANN dans les évaluations préliminaires de susceptibilité aux glissements de terrain.

Mots clés Glissement de terrain · SIG · Réseaux de neurones artificiels · Koyulhisar

Introduction

National and local government agencies are concerned with the loss of human life and damage to property caused by natural disasters such as hurricanes, earthquakes, erosion, tsunamis and landslides. Landslides accounted for approximately 9% of the natural disasters which occurred worldwide during the 1990s. Of all geological risks, landslides are among those that cause most damage, producing thousands of deaths every year and material losses of billions of dollars (Brabb 1991). According to Schuster (1996), this trend is expected to continue in the next decades due to increased urbanization and development, continued deforestation and increased regional precipitation in landslide-prone areas due to changing climatic patterns.

Many landslides are natural phenomena that occur independent of any human activities but others which resulted in serious losses have been induced by actions taken to make the land suitable for some human purpose. A number of workers have considered how to reduce losses due to landslides, based on maps of susceptibility, danger

I. Yilmaz (✉)
Department of Geological Engineering,
Faculty of Engineering, Cumhuriyet University,
58140 Sivas, Turkey
e-mail: iyilmaz@cumhuriyet.edu.tr

and risk (Ayala 1987; Coraminas 1987; Chacón et al. 1992, 1994, 1996). These maps are elaborated by means of deterministic and non-deterministic (probabilistic) models. The probabilistic methods are most frequently used and a large number of methodologies have been developed (Rengers et al. 1998), based on the inventory of landslides, geomorphological analysis, qualitative and statistical bivariate analysis (Brabb et al. 1972; Degraff and Romesburg 1980; Jade and Sarkar 1993; Irigaray 1995; Fernández et al. 2003; Yilmaz and Yildirim 2006) and multivariate analysis (Carrara 1983; Carrara et al. 1991; Baeza 1994; Chung et al. 1995). Many researchers have used different techniques such as heuristic approach (Ives and Messerli 1981; Rupke et al. 1988; Barredo et al. 2000; Van Westen et al. 2000; Van Westen and Lulie 2003), deterministic models (Ward et al. 1982; Cascini et al. 1991; Gokceoglu and Aksoy 1996), and statistical methods (Van Westen 1993; Chacón et al. 1994, 1996; Chung and Fabbri 1999; Dai et al. 2001; Lee and Min 2001; Carrara et al. 2003). Because of the deficiencies centered around the pore water pressure development in the soils and their spatial and temporal distribution, some physically based models have also been developed (Hammond et al. 1992; Montgomery and Dietrich 1994; Pack et al. 1998).

Quantitative techniques have become very popular in the last decades due to the developments in computer and GIS technology. The main problem with heuristic methods is that of insufficient knowledge about the area of interest, which sometimes leads to unacceptable generalizations. Other limitations of this method are the reproducibility of the results and the subjectivity of the weighting of the variables. Quantitative methods (deterministic) involve the estimation of quantitative values of stability variables, known as safety factors, over a defined area. They are only applied to areas where the landslide types are simple and the intrinsic properties are fairly homogeneous (Turner and Jayaprakash 1996). The required data include soil strength, depth below the terrain surface, soil layer thickness, slope angle and pore water pressure. These methods have been employed in translational landslides studies (Ward et al. 1982) and are only applicable at a large scale over small areas. One of the main drawbacks of these methods is their high degree of oversimplification when the data are incomplete. Another problem is that the data requirements for deterministic models can be prohibitive, and frequently it is impossible to acquire the input data necessary to use the model effectively (Gomez and Kavzoglu 2005).

In view of these drawbacks, such techniques as fuzzy-logic, artificial neural network (ANN) and neuro-fuzzy models have also been used to evaluate landslide susceptibility (Juang et al. 1992; Davis and Keller 1997; Binaghi et al. 1998; Gorsevski et al. 2003; Tangestani 2003; Ercanoglu and Gokceoglu 2004). Lu and Rosembaum (2003), Lee et al. (2003, 2004), Gomez and Kavzoglu (2005); Yesilnacar and Topal (2005); Yilmaz and Keskin (2007) discuss the use of ANN.

Landslides have different mechanisms and occur in different geological, morphological, and hydrological conditions. This paper discusses the use of an ANN model to produce a landslide susceptibility map for Koyulhisar (Sivas-Turkey), near the North Anatolian Fault Zone (Fig. 1).

Study area and landslides

The highland area of Koyulhisar (Fig. 2) includes the Boztepe, Saytepe and Igdir Mountains which rise to 1,361, 1,240 and 1,850 m, respectively. The slope angle in the study area varies from 20° to 75°. The main fault passing through the study area is the North Anatolian Fault, which extends NW-SE. In addition, the right-lateral Dumanlıca and Şıhlar fault and left-lateral Çamlıyaka faults cross the area (Fig. 2). The rocks are intensively fractured and two to four sets of joints have been recognized with extensions ranging from a few centimetres to tens of metres (Sendir and Yilmaz 2002).

The rocks outcropping in the landslide area consist of Pliocene volcanics, the Eocene Yesilce Formation and limestones of Maestrichtian age. These rocks are overlain by younger colluvium—essentially loose materials broken away from the bedrock. Thinly-bedded, whitish yellow and pink, crushed and jointed limestone is the oldest unit in the study area. The Yesilce Formation consists of conglomerates, sandy-gravelly limestone, andesite, basalts and pyroclastics (Terlemez and Yılmaz 1980). The jointed and massive Erdembaba volcanics comprises dacite, andesite and basalts. Slopes in the study area are partly covered by soil material varying in thickness from 0.5 to 2–3 m (Sendir and Yilmaz 2002).

Rainfall is the most important element in the hydrological cycle, with a mean annual precipitation of 394.6 mm (minimum 265.9 mm, 1962; maximum 575.1 mm, 1983).

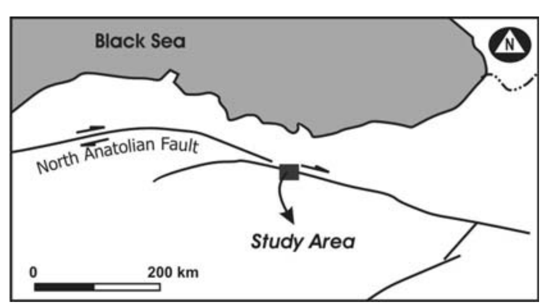

Fig. 1 Location map of the study area

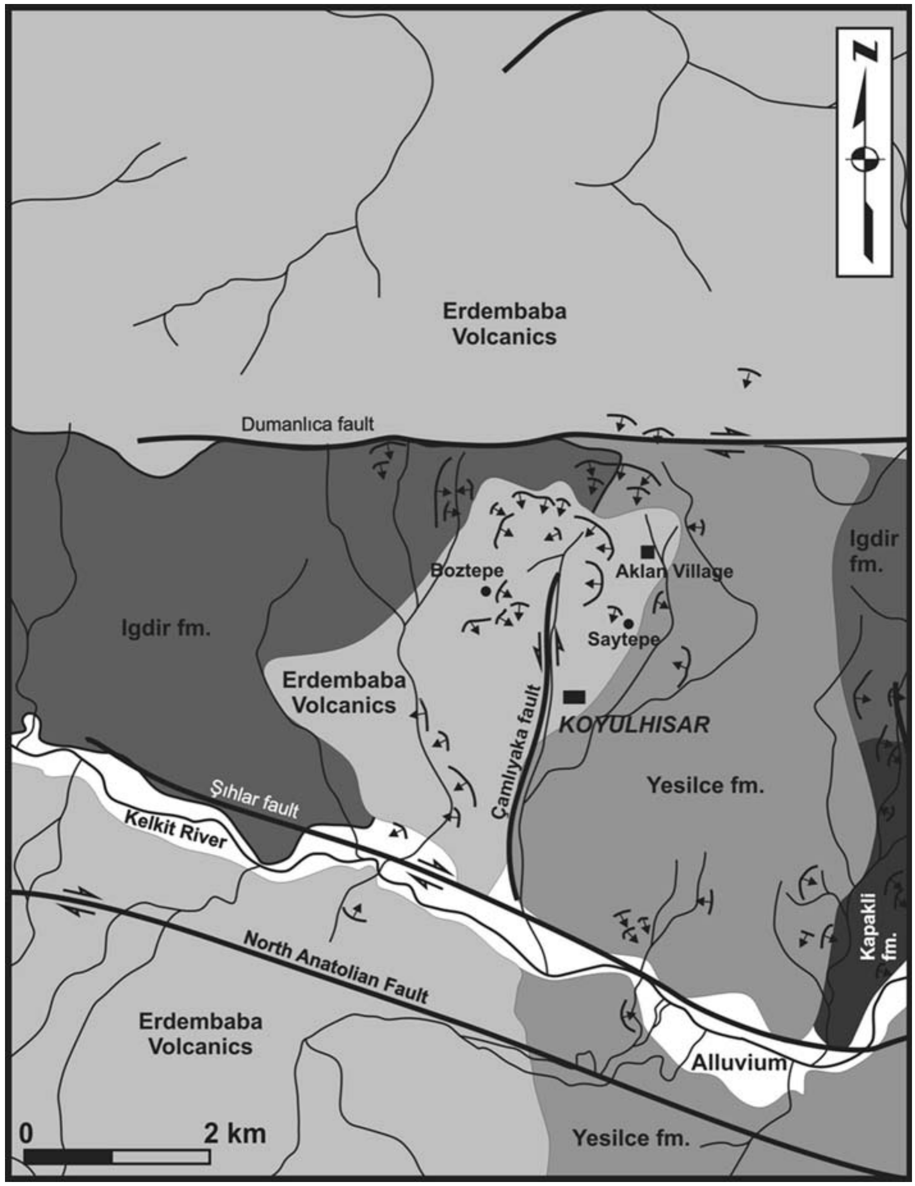

Fig. 2 Geological map of the study area

Most rainfall occurs during May (mean 64.4 mm). Meteorological records for 37 years show that the mean maximum temperature in August is 20.6°C; the mean minimum temperature is always recorded in January and is −1.9°C. Unfortunately the meteorological station was closed in 1992 hence no up-to-date information is available, but local people report that the wettest periods in memory were at the time of the large landslides which occurred on 19 August 1998 and 20 June 2000.

Landslides generally occur after the wet winter season, causing debris flows throughout northern Koyulhisar (Sendir and Yilmaz 2002; Yilmaz et al. 2005). The 19 August 1998 landslide covered an area of 1.5 km^2 and had an approximate volume of 400,000 m^3. The Aklan creek (some 2 km from Koyulhisar) was completely filled by debris within 24 h. Fortunately, the 1,240 m high Saytepe hill to the north of Koyulhisar protected the village. After 2 days, movement stopped and new tension cracks started to appear at the back of the main slip. The main tension crack extended with time and reached about 150 m in length and 1–1.5 m in width. On 20 June 2000, a new crack was observed in the slope 250–300 m above the backscar of the previous slip. During the morning of 21 June 2000, the area was involved in renewed movement which resulted in the destruction of some houses. Continuous monitoring of the slide area from 19 August 1998 until 15 May 2000 has shown an approximate total of 2.5 m of movement has occurred.

The landslides in the study area were classified as mainly rotational, although flow and complex landslides have been recorded. In some cases they are very deep and in others relatively shallow/surficial; in this study, the limited number of surficial/flow landslides were not taken into account.

Landslide susceptibility mapping

A digital elevation model (DEM) was first created using the 1:25,000 scale topographic maps (Fig. 3). It involved 1,308 rows and 1,006 columns, i.e. 1,315,848 cells (10 m × 10 m) enclosing a rectangle of ~131.6 km^2. The landslide locations and affected areas were plotted on the 1:25,000 scale topographic map using the Landsat TM satellite images (May 2006) and 1:35,000 aerial photographs; the information being completed and confirmed by field surveys. Factors considered in calculating the probability of landsliding were extracted from the constructed spatial database and transformed into a vector type spatial database using the GIS software of ArcGIS 9.1 (2005).

Many factors influence the occurrence of landslides, including geological, morphological, hydrogeological and meteorological conditions, vegetation and land-use. The intensity of precipitation was ignored in this study, because it was almost same in the whole area.

In this study ArcGIS 9.1 was used as a basic tool for spatial management and data manipulation and it was

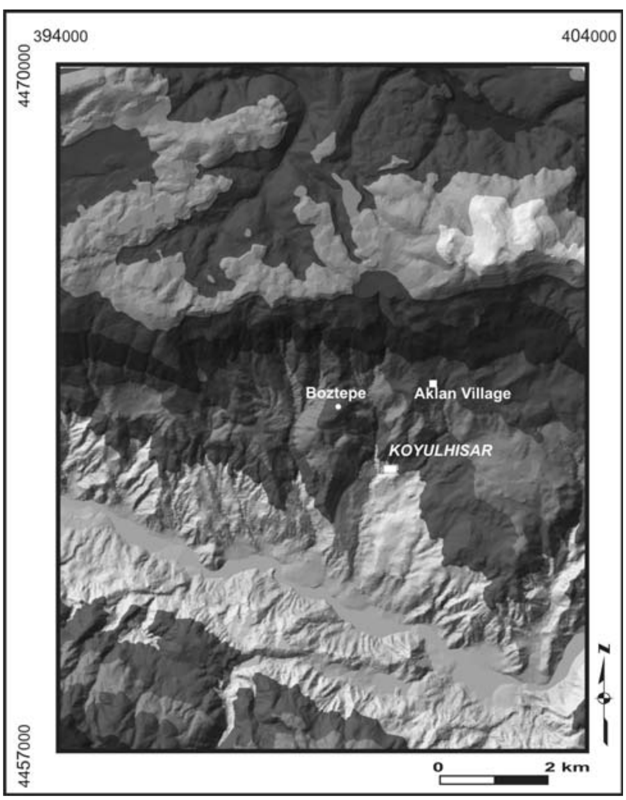

Fig. 3 Digital elevation model (DEM) of the study area

assumed that future landslides will occur under the same conditions as past landslides (Lee and Talib 2005). Frequency ratio was used for calculating the rating of the relative importance of each factor class to landslide occurrence (Table 1). The following parameters were used in the analyses.

1. Geological parameters:
   a. Lithology,
   b. Structural elements (distance from faults) (Fig. 4a).
2. Topographical parameters:
   a. Slope angle and aspect (Fig. 4b, c),
   b. Topographical elevation (Fig. 4d),
   c. Distance from drainage (Fig. 4e),
   d. Topographic wetness index (TWI) (Fig. 4f),
   e. Stream power index (SPI) (Fig. 4g).
3. Environmental parameters:
   a. Vegetation cover (Normalized Difference Vegetation Index (NDVI) (Fig. 4h),
   b. Distance from roads (Fig. 4i).

Neural networks may be used as a direct substitute for auto correlation, multivariable regression, linear regression, trigonometric and other statistical analysis and techniques (Singh et al. 2003) as they have a remarkable ability to derive meaning from complicated or imprecise data, extracting patterns and detecting complex trends. Trained neural networks can be thought of as an "expert" in the category of information it has been given to analyze, provide projections to new situations and answering "what if" questions. Other advantages include: adaptive learning, self-organization, real time operation and fault tolerance via redundant information coding.

A particular network can be defined using three fundamental components: transfer function, network architecture and learning law (Simpson 1990). It is essential to define these components, to solve the problem satisfactorily. Gomez and Kavzoglu (2005) suggested the use of ANNs as a method for landslide risk zonation as they can handle imprecise and fuzzy data as well as working with continuous, categorical and binary data without violating any assumptions.

Neural networks consist of a large class of different architectures. In many cases, the issue is approximating a static nonlinear, mapping $f(\mathbf{x})$ with a neural network $f(\mathbf{x})_{\mathbf{NN}}$, where $\mathbf{x} \in \mathbf{R}^{\mathbf{K}}$. There are many kinds of ANN models, among which the back propagation (BP) model is the most widely used. In this paper, a back propagation algorithm, created by generalizing the Widrow–Hoff learning rule to multiple-layer networks and nonlinear differentiable

Table 1 Frequency ratio of factors to landslide occurrences

Class	LSA (%) (a)	Grid (%) (b)	FR (a)/(b)
Geology			
Kapaklı fm.	6.55	2.23	2.94
Aluvvium	0.88	4.24	0.21
Volcanics	40.76	60.37	0.68
Igdir fm.	25.99	14.78	1.76
Yesilce fm.	25.81	18.38	1.40
Distance from fault			
0–250	10.03	13.29	0.75
250–500	32.56	13.30	2.45
500–750	26.46	12.59	2.10
750–1,000	15.10	10.03	1.51
1,000–1,250	4.48	9.32	0.48
1,250–1,500	3.82	8.91	0.43
1,500–1,750	7.54	8.10	0.93
1,750–2,000	0.01	6.50	0.00
2,000–2,250	0.00	5.82	0.00
2,250–4,806	0.00	12.14	0.00
Distance from drainage			
0–150	25.32	22.80	1.11
150–300	30.77	20.49	1.50
300–450	21.14	15.86	1.33
450–600	11.07	10.73	1.03
600–750	9.33	9.09	1.03
750–900	2.36	6.77	0.35
900–1,050	0.01	5.81	0.00
1,050–1,200	0.00	4.03	0.00
1,200–1,350	0.00	2.27	0.00
1,350–2,097	0.00	2.15	0.00
Topographical elevation			
630–780	9.16	14.58	0.63
780–930	12.07	12.76	0.95
930–1,080	7.93	11.34	0.70
1,080–1,230	17.80	9.14	1.95
1,230–1,380	22.32	7.30	3.06
1,380–1,530	20.08	5.37	3.74
1,530–1,680	9.89	14.26	0.69
1,680–1,830	0.74	21.49	0.03
1,830–1,980	0.00	2.77	0.00
1,980–2,030	0.00	0.99	0.00
Distance to roads			
0–250	9.73	15.61	0.62
250–500	22.01	11.64	1.89
500–750	13.74	9.01	1.53
750–1,000	18.38	12.92	1.42
1,000–1,250	10.89	7.80	1.40
1,250–1,500	12.71	8.61	1.48
1,500–1,750	5.97	5.42	1.10
1,750–2,000	4.62	4.27	1.08
2,000–2,250	1.96	3.68	0.53
2,250–5,203	0.00	21.05	0.00

Table 1 continued

Class	LSA (%) (a)	Grid (%) (b)	FR (a)/(b)
Slope			
0–7	5.17	21.04	0.25
7–14	20.01	26.56	0.75
14–21	22.94	23.30	0.98
21–28	22.02	15.35	1.43
28–35	15.81	8.86	1.79
35–42	11.83	3.76	3.14
42–49	1.87	0.61	3.09
49–56	0.28	0.10	2.77
56–63	0.05	0.07	0.72
63–89	0.01	0.34	0.03
Aspect			
Flat	1.84	13.33	0.14
N	0.53	5.44	0.10
NE	4.86	9.17	0.53
E	13.47	8.86	1.52
SE	19.09	10.70	1.78
S	28.32	16.34	1.73
SW	16.72	13.87	1.21
W	10.85	9.27	1.17
NW	3.81	8.12	0.47
N	0.51	4.91	0.10
TWI			
0.11–1.38	38.07	21.90	1.74
1.39–1.85	31.81	27.20	1.17
1.86–2.33	16.41	22.77	0.72
2.34–2.81	9.58	14.94	0.64
2.82–2.39	3.66	7.00	0.52
2.40–4.07	0.22	2.68	0.08
4.08–4.98	0.18	2.26	0.08
4.99–6.14	0.04	0.57	0.07
6.15–7.83	0.02	0.47	0.05
7.84–13.60	0.00	0.21	0.00
SPI			
0–750	5.88	22.75	0.26
750–1,500	22.69	28.64	0.79
1,500–2,250	25.33	23.42	1.08
2,250–3,000	20.99	14.63	1.43
3,000–3,750	17.01	7.41	2.30
3,750–4,500	7.18	2.30	3.12
4,500–5,250	0.78	0.31	2.50
5,250–6,000	0.11	0.07	1.43
6,000–6,750	0.03	0.17	0.19
6,750–8,879	0.00	0.29	0.00
NDVI			
−0.9–0.1	33.84	31.52	1.07
0.1–0.3	21.55	23.48	0.92
0.3–0.6	43.08	39.64	1.09
0.6–0.83	1.53	5.36	0.29

LSA landslide affected grid percent in range or type, *Grid* grid percent of range/type in whole area, FR: frequency ratio

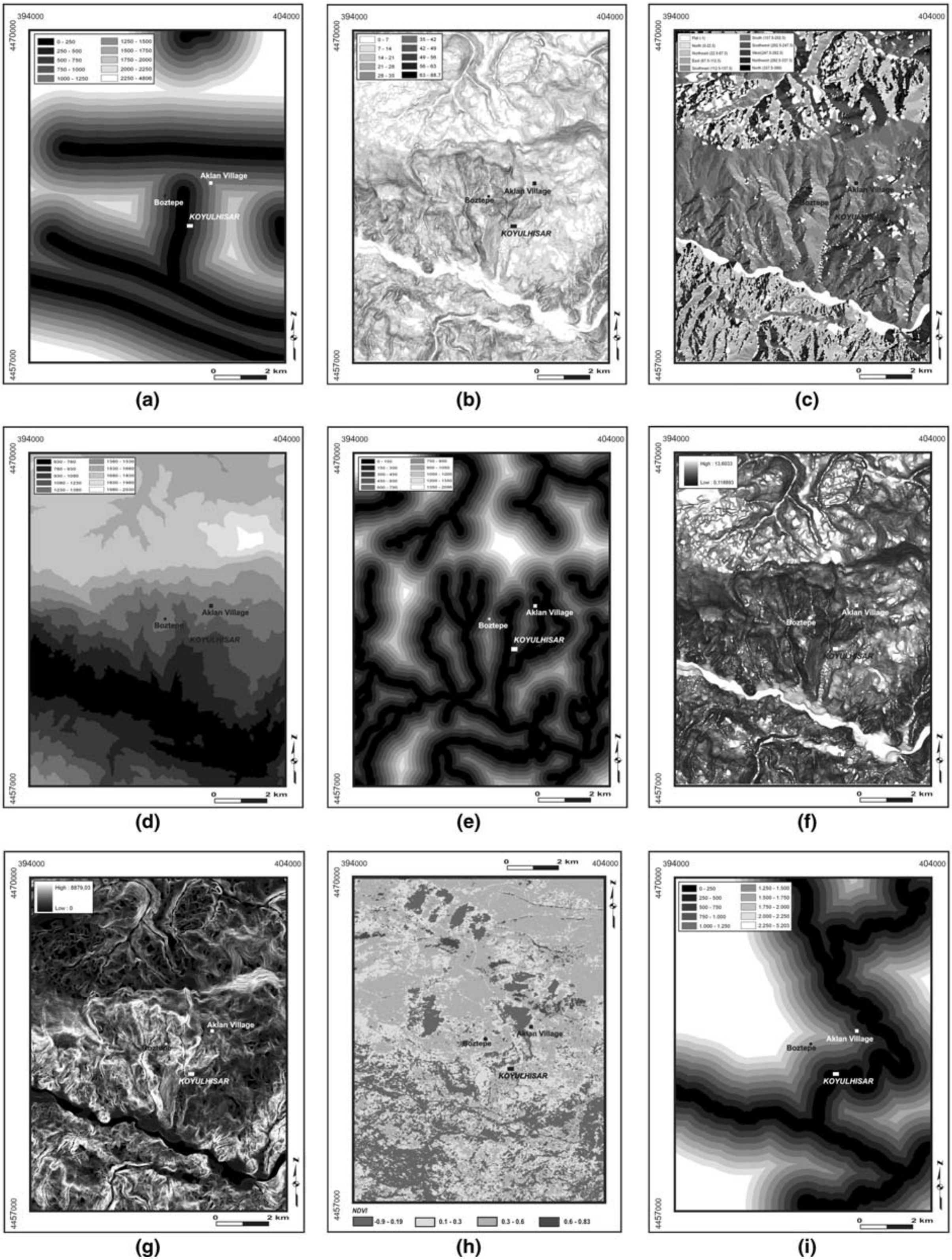

Fig. 4 **a** Distance from faults. **b** Slope map. **c** Slope aspect map. **d** Topographical elevation map. **e** Distance from drainage. **f** TWI map. **g** SPI map. **h** NDVI map. **i** Distance from main roads

transfer function, was used. A back propagation consists of an input layer, several hidden layers and output layers, all of which may contain multiple nodes (After Yilmaz and Yüksek 2007).

The inputs x_n, $n = 1, \ldots, n$ to the neuron are multiplied by weights w_{ni} and summed with the constant bias term Q_i. The resulting n_i is the input to the activation function y. The activation function was originally chosen to be a relay function, but for mathematical convenience a hyperbolic tangent (tanh) or a sigmoid function are most commonly used. The hyperbolic tangent is defined as

$$f(x) = \tanh(x) = \frac{e^x - e^{-x}}{e^x + e^{-x}} \tag{1}$$

The output of node i becomes

$$y_i = f\left(\sum_{j=1}^{k} w_{ik} x_j + Q_i\right) \tag{2}$$

Connecting several nodes in parallel and series, a MLP network is formed. A typical network is shown in Fig. 5. The following equations explain the mathematical notation of the back propagation algorithm.

$$net_i = \sum_{\forall j w_{ji} \neq 0} w_{ji} * a_j \tag{3}$$

$$a_i = \frac{1}{1 + e^{-\mathrm{net}_i}} \tag{4}$$

$$E_p = \sum_{i \in \text{Output units}} (a_i - o_i)^2 \tag{5}$$

$$E = \sum_p E_p \tag{6}$$

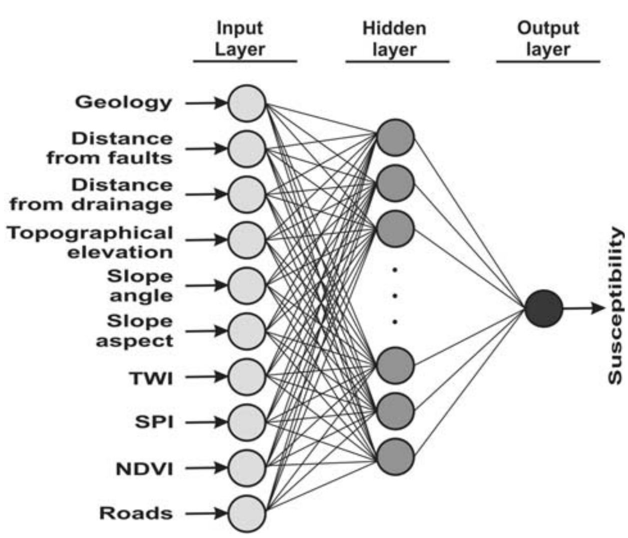

Fig. 5 Neural network structure used in the study

Partial derivative for pattern p with respect to w_{ij}:

$$\frac{\partial E_p}{\partial w_{ij}} \tag{7}$$

Partial derivative for the whole training set with respect to w_{ij}:

$$\frac{\partial E}{\partial w_{ij}} \tag{8}$$

$$\frac{\partial E}{\partial_{w_{ij}}} = \sum_p \frac{\partial E_p}{\partial w_{ij}} \tag{9}$$

$$\nabla E = \frac{\partial E}{\partial_{w1}}, \frac{\partial E}{\partial_{w2}}, \ldots, \frac{\partial E}{\partial_{wn}} \tag{10}$$

$$\nabla E_p = \frac{\partial E_p}{\partial_{w1}}, \frac{\partial E_p}{\partial_{w2}}, \ldots, \frac{\partial E_p}{\partial_{wn}} \tag{11}$$

$$w_{ij}(n+1) = \Delta w_{ij}(n) + w_{ij}(n) \tag{12}$$

In Eqs. 3–12; a_i: activation of unit i, w_{ij}: connection strength from unit i to unit j, o_i: desired activation of output unit i (ith's component of the output vector), net_i: net input to unit i, E_p: quadratic error for pattern p, E: total quadratic error on the training set, ∇E: gradient with respect to the whole training sets, ∇E: gradient with respect to pattern p, $\Delta w_{ij}(n)$: weight update of w_{ij} in the nth learning step.

The learning is done using the following procedure:

1. Selection of random and small sized (between 0 and 1) numbers for all weights and bias.
2. Calculation of network output and comparison with the destination output.
3. If the network output is approximately equal to the desired output, then continue with step 1, and if not weights are corrected according to the correction rule.

MatLab 7.0 was used for training and testing the neural networks. A three-layer feed-forward network consisting of an input layer (10 neurons), one hidden layer (21 neurons) and one output layer was used as a network structure of 10-21-1 (Fig. 5). In order to find the number of hidden layer nodes, Eq. 13 proposed by Hecht-Nielsen (1987) was used.

$$N_h = 2 * N_i + 1 \tag{13}$$

where N_i is the number of input nodes and N_h is the number of hidden nodes.

Initial weight range is also an important parameter influencing the convergence of learning rule. In this study, weights were randomly initialized in a small range of [−0.25 to 0.25] as proposed by Kavzoglu (2001), who also suggested that the minimum number of training samples should be more than $30*N_i*(N_i + 1)$ where N_i is the number of input nodes. Learning and momentum parameters were set as proposed by Foody et al. (1996). Five thousand two fifty pixels were randomly selected from the two classes (landslide and non-landslide) as training samples, and parameters were then adjusted as below:

Learning parameters: 0.1
Momentum parameters: 0.9
Networks training function: variable learning rate with momentum (traingdx)
Activation (transfer) function for all layers: tansig

The training areas were checked in the field for accuracy and completeness. As in many other network training methods, models and parameters were used in order to reach the minimum root mean square error (RMSE) values. The RMSE goal for stopping was 0.1. After the network goal was reached, the whole study area was fed into the network in order to estimate the landslide susceptibility. The set of susceptibility values obtained in each grid were then converted to a raster file in GIS medium and a landslide susceptibility map was produced (Fig. 6).

The values of LSI were classified using equal areas. The proportions were sorted from the smallest to the largest and divided into five groups to represent the relative susceptibility. To ensure that the points used to define the five groups were determined objectively, a non-hierarchical cluster analysis was used (Yilmaz 2007).

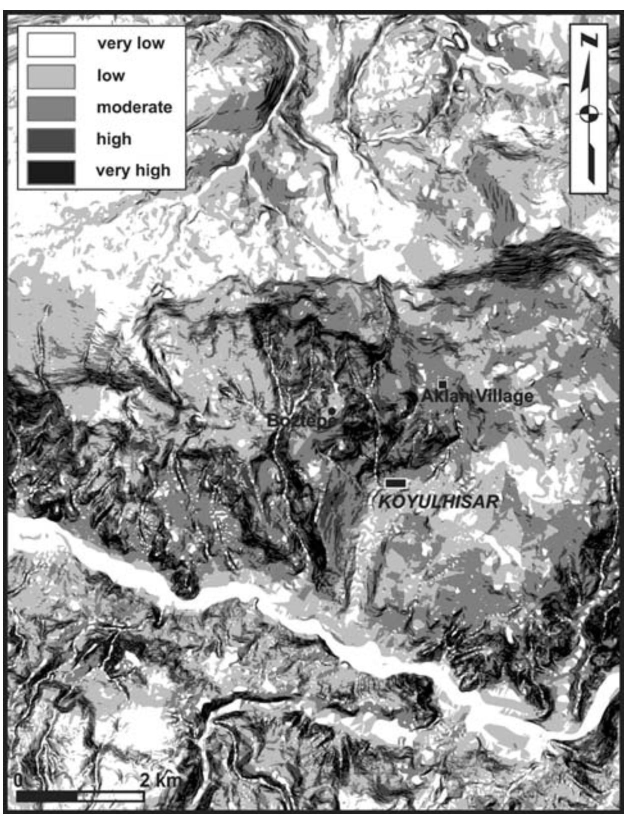

Fig. 6 Landslide susceptibility map produced from ANN model

The initial division into the five groups was achieved by breaking the range of proportional values equally. The upper and lower boundaries of each group were retained or adjusted to ensure that the final division represented the minimum sum of the squared deviations around the four group means. This is based on the W function (Anderberg 1973).

Validation of the model used

Two procedures for validation of the map were used: the area under curve (AUC) method proposed by Lee and Talib (2005) and the degree of fit (DF) method put forward by (Irigaray 1995). Lee and Talib (2005) report that the AUC is a good indicator to check the prediction performance of the model with an AUC varying from 0.5 to 1.0 being the ideal. To obtain the rate curve, the calculated landslide susceptibility index values of all grids in the study area were first sorted and the ordered grid values then divided into 100 classes at 1% intervals (Fig. 7). The AUC value of the ANN model produced was calculated as 84.7% implying an accurate map. The degree of fit (Irigaray 1995) was calculated by use of the following equation.

$$DF = \frac{z_i/S_i}{\sum z_i/S_i} \tag{14}$$

where z_i: area of affected by landslide in the i class of susceptibility, S_i: area of the i class of susceptibility. Figure 8 illustrates the degrees of fit and indicated a very high quality of map had been produced.

Discussion and conclusions

Landslide susceptibility can be assessed using different methods based on GIS technology. Especially in the last twenty years, much research work has been undertaken to solve the deficiencies and difficulties in the assessment of susceptibility and create a procedure for preparing

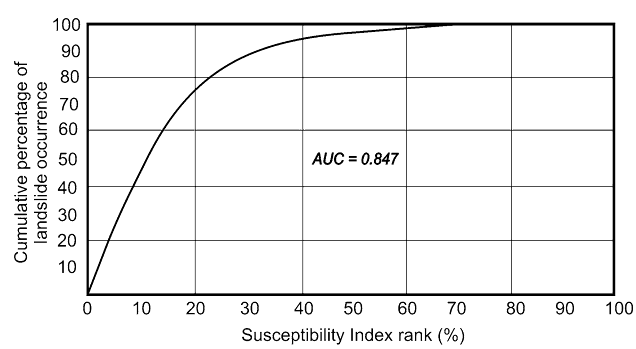

Fig. 7 AUC representing the quality of the model used

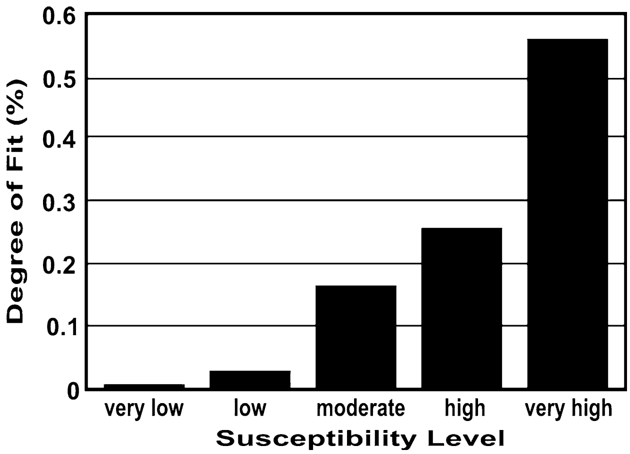

Fig. 8 Degree of fit of susceptibility classes

landslide susceptibility map which is both simple and with a high degree of accuracy.

The results obtained in this study showed that the ANN can be used as a precise tool in the assessment of the landslide susceptibility when a sufficient number of data are available. The main problem with the use of ANN is that the input process, calculations, output process and training stage of the network are time-consuming. In addition, neural networks require a conversion of data used in the analyses into ASCII or other formats and it is very hard to process the large amount of data.

The validation procedures used showed the susceptibility map produced in this study was of high quality hence the method may be helpful for planners and engineers, although it is recommended it is used for generalized planning and assessment purposes only.

References

Anderberg MR (1973) Cluster analysis for applications. Academic Press, New York

ArcGIS (Version 9.1), 2005. Integrated GIS Software. ESRI, CA

Ayala FJ (1987) Introducción a los riesgos geológicos. In: Ayala FJ (ed) Riesgos Geológicos, IGME, Serie Geología Ambiental. Madrid, Spain, pp 3–19

Baeza C (1994) Evaluación de las condiciones de rotura y la movilidad de los deslizamientos superficiales mediante el uso de técnicas de análisis multivariante, Tesis Univ Pol Catalunya

Barredo JJ, Benavides A, Hervas J, Van Westen CJ (2000) Comparing heuristic landslide hazard assessment techniques using GIS in the Trijana basin, Gran Canaria Island, Spain. JAG 2(1):9–23

Binaghi E, Luzi L, Madella P, Rampini A (1998) Slope instability zonation: a comparison between certainty factor and fuzzy Dempster-Shafer approaches. Nat Hazards 17:77–97

Brabb EE (1991) The world landslide problem. Episodes 14(1):52–61

Brabb EE, Pampeyan EH, Bonilla M (1972) Landslide Susceptibility in the San Mateo County, California, scale 1:62.500, U.S.G.S. Misc. Field Studies Map MF344

Carrara A (1983) Multivariate models for landslide hazard evaluation. Math Geol 15(3):403–426

Carrara A, Cardinalli M, Detti R, Guzzetti F, Pasqui V, Reichenbach P (1991) GİS techniques and statitistical models in evaluating landslide hazards. Earth Surf Process Landf 16:427–445

Carrara A, Crosta G, Frattini P (2003) Geomorphological and historical data in assessing landslide hazard. Earth Surf Process Landf 28:1125–1142

Cascini L, Critelli S, Gulla G, Di Nocera S (1991) A methodological approach to landslide hazard assessment: a case history. In: Proceedings of 16th international landslide conference. Balkema, Rotterdam, pp 899–904

Chacón J, Irigaray C, Fenandez T (1992) Metodologia para la cartografia regianal de movientos de ladera y riesgos asociados mediante un Sistema de Informacions Geografica. In: Corominas J, Alonso E (eds) III Simposio Nacional sobre Taludes y laderas Inesstables. vol. I. La Corruna, Spain, pp 121–133

Chacón J, Irigaray C, Fernández T (1994) Large to middle scale landslide inventory, analysis and mapping with modelling and assessment of derived susceptibility, hazards and risks in a GIS. In: Proceedings of 7th IAEG congress, Balkema, Rotterdam, pp 4669–4678

Chacón J, Irigaray C, Fernández T (1996) From the inventory to the risk analysis: Improvements to a large scale GIS method. In: Chacón J, Irigaray C, Fernández T (eds) Proceedings of 8th international conference. and field workshop on landslides, Balkema, pp 335–342

Chung CF, Fabbri AG (1999) Probabilistic prediction models for landslide hazard mapping. Photogramm Eng & Remote Sens 65(12):1389–1399

Chung CF, Fabbri AG, van Westen CJ (1995) Multivariate regression analysis for landslide hazard zonalition. In: Carrara A, Guzetti F (eds) Geographical informations systems in assessing natural hazards. Kluwer, Dordrecht

Coraminas J (1987) Criterios para la confeccion de mapes de peligrosidad de movimentos de ladera. In: Ayala FJ (ed) Riesgos Geologicos, IGME Serie Geologia Ambiental. Madrid, Spain, pp 193–201

Dai FC, Lee CF, Zhang XH (2001) GIS-based geo-environmental evaluation for urban land-use planning: a case study. Eng Geol 61:257–271

Davis TJ, Keller CP (1997) Modelling uncertainty in natural resource analysis using fuzzy sets and Monte-Carlo simulation: slope instability prediction. Int J Geogr Inf Sci 11(5):409–434

DeGraff J, Romesburg H (1980) Regional landslide-susceptibility assessment for wildland management: a matrix approach. In: Coates D, Vitek J (eds) Thresholds in geomorphology. George Allen and Unwin, London, pp 401–414

Ercanoglu M, Gokceoglu C (2004) Use of fuzzy relations to produce landslide susceptibility map of a landslide prone area (West Black Sea Region Turkey). Eng Geol 75:229–250

Fernández T, Irigaray C, Hamdouni RE, Chacón J (2003) Methodology for landslide susceptibility mapping by means of a GIS. Application to the contraviesa area (Granada, Spain). Nat Hazards 30:297–308

Foody GM, Lucas RM, Curran PJ, Honzak M (1996) Estimation of the areal extend of land cover classes that only occur at a sub-pixel level. Can J Remote Sens 22:432–438

Gokceoglu C, Aksoy H (1996) Landslide susceptibility mapping of the slopes in the residual soils of the Mengen region (Turkey) by deterministic stability analyses and image processing technique. Eng Geol 44:147–161

Gomez H, Kavzoglu T (2005) Assessment of shallow landslide susceptibility using artificial neural networks in Jabonosa River Basin, Venezuela. Eng Geol 78(1–2):11–27

Gorsevski PV, Gessler PE, Jankowski P (2003) Integrating a fuzzy k-means classification and a Bayesian approach for spatial prediction of landslide hazard. J Geogr Syst 5(3):223–251

Hammond C, Hall D, Miller S, Swetik P (1992) Level I Stability Analysis (LISA) Documentation Version 2.0, General Technical Report INT-285. United States Department of Agriculture, Forest Service Intermountain Research Station, USA
Hecht-Nielsen R (1987) Kolmogorov's mapping neural network existence theorem. In: Proceedings of 1st IEEE international conference on neural networks, San Diego, pp 11–14
Irigaray C (1995) Movimientos de ladera: inventoria, analisis y cartografaa de susceptibilidad mediante un Sistema de Informacion Geografica. Aplicacion a las zonas de Colmenar (Ma), Rute (Co) y Montefrio (Gr). Thesis Doctoral, University Granada
Ives JD, Messerli B (1981) Mountain hazard mapping in Nepal: introduction to an applied mountain research project. Mt Res Dev 1(3–4):223–230
Jade S, Sarkar S (1993) Statistical models for slope instability classification. Eng Geol 36:91–98
Juang CH, Lee DH, Sheu C (1992) Mapping slope failure potential using fuzzy sets. J Geotech Eng, ASCE 118(3):475–493
Kavzoglu T (2001) An investigation of the design and use of feed-forward artificial neural networks in the classification of remotely sensed images. Ph.D. thesis, University of Nottingham, School of Geography, 306 p
Lee S, Min K (2001) Statistical analyses of landslide susceptibility at Yongin. Korea Environ Geol 40:1095–1113
Lee S, Talib JA (2005) Probabilistic landslide susceptibility and factor effect analysis. Environ Geol 47:982–990
Lee S, Ryu JH, Min K, Won JS (2003) Landslide susceptibility analysis using GIS and artificial neural network. Earth Surf Proc Land 28(12):1361–1376
Lee S, Ryu JH, Won JS, Park HJ (2004) Determination and application of the weights for landslide susceptibility mapping using an artificial neural network. Eng Geol 71:289–302
Lu P, Rosembaum MS (2003) Artificial neural networks and grey systems for the prediction of slope instability. Nat Hazards 30(3):383–398
Montgomery DR, Dietrich WE (1994) A physically based model for the topographic control on shallow landsliding. Water Resour Res 30(4):1153–1171
Pack RT, Tarboton DG, Goodwin CN (1998) Terrain Stability Mapping with SINMAP, technical description and users guide for version 1.00, Report Number 4114-0, Terratech Consulting Ltd., Salmon Arm, BC., Canada (www.tclbc.com)
Rengers N, van Westen CJ, Chacón J, Irigaray C (1998) Draft for the chapter on the application of digital techniques for natural hazard zonation, Report on Mapping of Natural Hazards, International Association of Engineering Geology. Commission No. 1 on Engineering Geological Mapping
Rupke J, Cammeraat E, Seijmonsbergen AC, Van Westen CJ (1988) Engineering geomorphology of the Widentobel catchment, Switzerland: a geomorphological inventory system applied to geotechnical appraisal of the slope stability. Eng Geol 26:33–68
Schuster R (1996) Socioeconomic significance of landslides. In: Turner AK, Schuster RL (eds) Landslides: investigation and mitigation: special report, vol 247. National Academic Press, Washington, pp 12–36
Sendir H, Yilmaz I (2002) Structural, geomorphological and geomechanical aspects of the Koyulhisar landslides in the North Anatolian Fault Zone (Sivas-Turkey). Env Geol 42(1):52–60
Simpson PK (1990) Artificial neural system-foundation, paradigm, application and implementation. Pergamon Press, New York
Singh TN, Kanchan R, Verma AK, Singh S (2003) An intelligent approach for prediction of triaxial properties using unconfined uniaxial strength. Min Eng J 5(4):12–16
Tangestani MH (2003) Landslide susceptibility mapping using fuzzy gamma operation in a GIS, Kakan catchment area, Iran. Map India 2003, Disaster Management, 7 p
Terlemez İ, Yılmaz A (1980) Ünye-Ordu-Reşadiye-Koyulhisar-Karaçayır-Hafik arasında kalan bölgenin jeolojisi. M.T.A. Report No. 6671. (in Turkish)
Turner K, Jayaprakash G (1996) Landslides: investigation and mitigation, introduction. In: Turner AK, Schuster RL (eds) Special report, vol. 247. National Academic Press, Washington, pp 3–12
Van Westen CJ (1993) Application of geographic information systems to landslide hazard zonation. Ph.D. dissertation Technical University Delft. ITC Publication Number 15, ITC, Enschede, The Netherlands, 245 p
Van Westen CJ, Lulie GF (2003) Analyzing the evolution of the Tessina landslide using aerial photographs and digital elevation models. Geomorphology 54(1–2):77–89
Van Westen CJ, Soeters R, Sijmons K (2000) Digital Geomorphological landslide hazard mapping of the Alpago area, Italy. Int J Appl Earth Obs Geoinf 2(1):51–59
Ward TJ, Ruh-Ming L, Simons DB (1982) Mapping landslide hazard in forest watershed. J Geotech Eng Div, ASCE 108 (GT-2): 319–324
Yesilnacar E, Topal T (2005) Landslide susceptibility mapping: a comparison of logistic regression and neural networks method in a medium scale study, Hendek region (Turkey). Eng Geol 79:251–266
Yilmaz I (2007) GIS based susceptibility mapping of karst depression in gypsum: a case study from Sivas basin (Turkey). Eng Geol 90:89–103
Yilmaz I, Keskin I (2007) Sebinkarahisar ve Alucra yöresi heyelanları: Heyelan duyarlılık haritalarının Frekans Oranı (FR) ve Yapay Sinir Ağları (ANN) Modelleri kullanılarak hazırlanması. Cumhuriyet University BAP Project Report, M-342, 90 p (in Turkish with English abstract)
Yilmaz I, Yildirim M (2006) Structural and geomorphological aspects of the Kat landslides (Tokat-Turkey), and susceptibility mapping by means of GIS. Env Geol 50(4):461–472
Yilmaz I, Yüksek AG (2007) An example of artificial neural network application for indirect estimation of rock parameters. Rock Mech Rock Eng 41(5):781–795
Yilmaz I, Ekemen T, Yıldırım M, Keskin I, Özdemir G (2005) Failure and flow development of a collapse induced complex landslide: the 2005 Kuzulu (Koyulhisar-Turkey) landslide hazard. Env Geol 49(3):467–476